Examining Fresh Water Flux over Global Oceans in the NCEP CDAS, CDAS2, GDAS,GFS, and CFS

P. Xie[1], J.E. Janowiak[2], M. Chen[1], W. Wang[1], C.-L. Shie[3], and L. Chiu[4]

[1] Climate Prediction Center, NOAA, U.S.A.

[2] Earth System Science Interdisciplinary Center, UMD, USA

[3] UMBC / Goddard Space Flight Center, NASA, U.S.A.

[4] Center for Earth Sciences and Space Research, GMU, U.S.A.

Correspondence: Pingping.Xie@noaa.gov

1. INTRODUCTION

Oceanic fresh water flux is an essential component of the global water cycle and plays an important role in forcing the oceanic circulation. However, its mean state, short-term variability and long-term changes are poorly monitored and documented due to undesirable quality of the data sets for its two primary components, precipitation (P) and evaporation (E). While fields of oceanic precipitation and evaporation are routinely generated by global models, their performance in reproducing spatial distribution and temporal variation patterns of fresh water flux needs to be examined before they may be utilized in various applications.

The objective of this paper is to assess the seasonal and interannual variations of oceanic fresh water flux produced by the NOAA National Centers for Environmental Prediction (NCEP) reanalyses and operational global models. Global fields of oceanic precipitation and evaporation are compared against corresponding observations with consideration of quantitative uncertainties inherent in the observations.

2. DATA

2.1 THE NCEP MODEL-BASED PRODUCTS

Oceanic precipitation and evaporation fields from five sets of NCEP model-based products are examined in this study. These include the Climate Data Assimilation System 1 (CDAS1, Kalnay et al. 1996), often called NCEP/NCAR Reanalysis1; the Climate Data Assimilation System 2 (CDAS2, Kanamitsu et al. 2002), also known as NCEP Reanalysis 2; the Global Data Assimilation System (GDAS) which is the NCEP operational systems that assimilates available in situ and satellite observations through the state-of-the-art models; the AMIP simulation of the Global Forecast System (GFS) global atmospheric model; and the CMIP simulations of the Climate Forecast System (CFS, Saha et al. 2006) that is a coupled global model with GFS and GFDL/MOM3 as its atmospheric and oceanic component, respectively.

2.2 THE OBSERVATION DATA SETS

One problem of using satellite-based oceanic precipitation and evaporation estimates to assess model-generated products is the bias of unknown magnitude inherent in the individual data sets. To reduce the uncertainty caused by this bias, multiple sets of precipitation / evaporation data sets are employed in the examinations in which the mean and standard deviation of these data sets are used to define the ‘truth’ of the fresh water fluxes and its uncertainty, respectively.

Satellite-based precipitation data sets utilized in this study to include the CPC Merged Analysis of Precipitation (CMAP, Xie and Arkin 1997), the Global Precipitation Climatology Project (GPCP) Version 2 merged analysis

(Adler et al. 2003), and the Tropical Rainfall Measurement Mission (TRMM) TMI-PR merged products. Monthly, seasonal and annual climatology of oceanic precipitation is defined for 1988-2000 for CMAP and GPCP, and for 1998-2006 for the TRMM data sets, respectively. The largest uncertainties in observed precipitation appear over the heavy rainfall ITCZ regions and over high-latitudes where CMAP and GPCP take different inputs to define their analyses (fig.1). Overall, the uncertainty, measured by the standard deviation among the individual climatologies, is about 10% of the mean precipitation values.

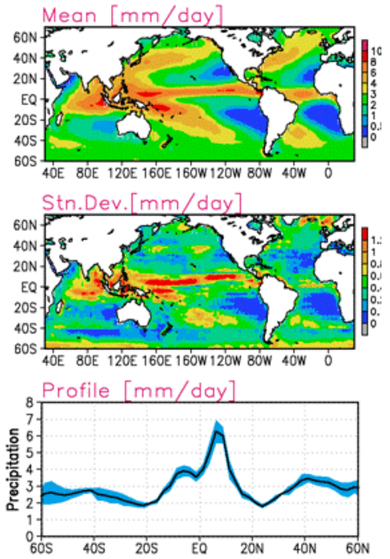

Fig. 1 Global distribution of the mean (upper) and standard deviation (middle), together with their zonal means (bottom), among the annual mean precipitation (mm/day) from the CMAP, GPCP, and TRMM TMI-PR merged Data sets.

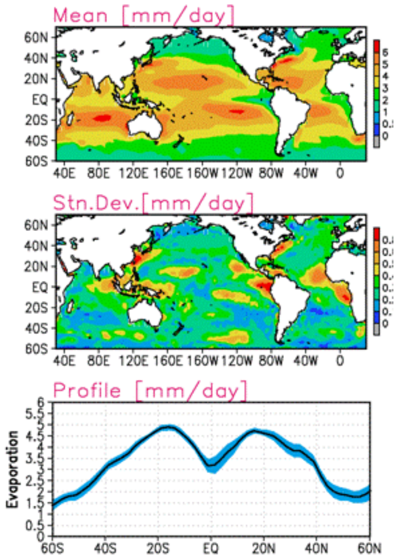

Fig. 2 Same as in figure 1, except for evaporations from four sets of observation data sets: the satellite-based GSSTF2, J-OFURO2, and HOAPS3, and the COADS-based SOC climatology.

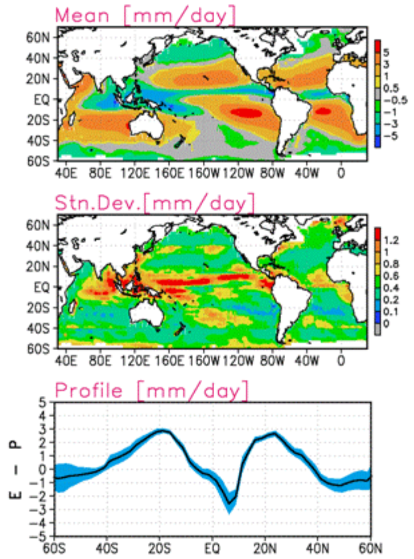

Fig.3: Same as in figure 1, except for the fresh water flux (Evaporation – precipitation, mm/day), from the combinations of the observed evaporation and precipitation data sets.

Four sets of observation-based data sets are used to define the ‘truth’ of oceanic evaporation. These include the Goddard Satellite-based Surface Turbulent Flux Version 2 (GSSTF2) of Chou et al. (2003), the Hamburg Ocean Atmosphere Parameters from satellite data Version 3 (HOAPS3) of Grassl et al. (2000), the Japanese Ocean Flux with Use of Remote Sensing Observation Version 2 (J-OFURO2) of Tomita et al. (2007), and the COADS-based Southapmton Oceangraphy Centre (SOC) climatology of Josey et al. (1998,1999). As shown in fig.2, maximum values of oceanic evaporation are observed over mid-latitudes, while large uncertainties of observed evaporation are located over equatorial tropical oceans and over coastal regions in NW Pacific and Atlantic Oceans. Overall, uncertainty is ~10% of observed mean evaporation over ocean. Combined, the observed long-tern mean of precipitation (P) and evaporation (E) presents net fresh water coming into / out of the ocean over the tropics / subtropics, respectively, with a quantitative uncertainty of 10-15% in the annual / seasonal mean climatology defined by the currently available observation data sets (fig.3).

3. SEASONAL VARIATIONS

Seasonal variations of global oceanic fresh water flux generated by the NCEP CDAS1, CDAS2, GDAS, GFS and CFS are examined against the observations described in the previous section. Annual and seasonal mean precipitation and evaporation is defined over 1988-2000 for the CDAS1 and CDAS2, over 2000-2006 for the GDAS, over 1981-2003 for the GFS and over 4 sets of 32-year periods for the CFS simulations, respectively.

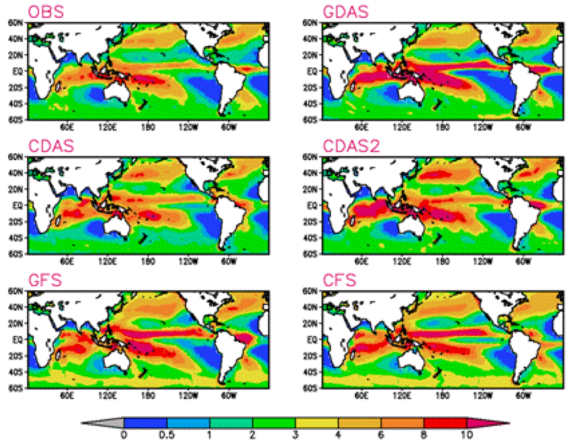

Fig.4 DJF mean precipitation (mm/day) defined from the observations (upper left), GDAS (upper right), CDAS1 (middle left), CDAS2 (middle right), GFS (bottom left), and CFS (bottom right).

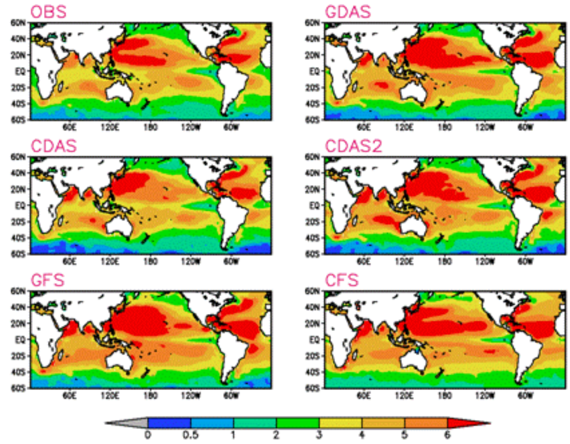

Fig.5: Same as in figure 4, except for DJF mean evaporation.

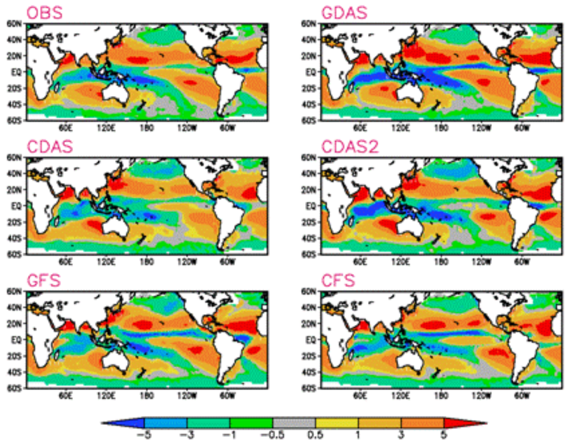

Fig.6 Same as in figure 4, except for DJF mean fresh Water flux (E-P).

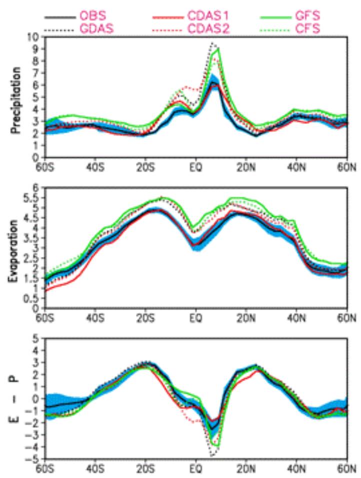

Fig.7 Latitudinal profile of annual averaged zonal mean precipitation (upper), evaporation (middle) and fresh water (bottom), derived from the observations and various NCEP products. The black line indicates the mean while blue spread shows the uncertainty of the observations.

Large-scale patterns of oceanic precipitation and evaporation are reasonably well reproduced by the NCEP global products examined here (fig.4-6). In particular, the spatial distribution (fig.4) and seasonal migration (not shown) of the ITCZ and SPCZ precipitation generated by the NCEP operational GDAS exhibits very close agreements with those in the observations. Overall, except the CDAS1, all of the NCEP products examined here produced global fields of precipitation and evaporation with excessive magnitude over most of the latitude bands (fig.7). The net fresh water flux in the NCEP products, however, is closer to the observations, except over tropics where excessive amount of precipitation generated by the CDAS2, GDAS, GFS and CFS is not canceled completely by the over-estimation for evaporation (fig.7,bottom).

4. INTERANNUAL VARIABILITY

Monthly anomaly fields of precipitation and evaporation generated by the NCEP products are compared to those of the observations to assess performance of the NCEP reanalyses and global models to reproduce the interannual variability of fresh water flux over oceans.

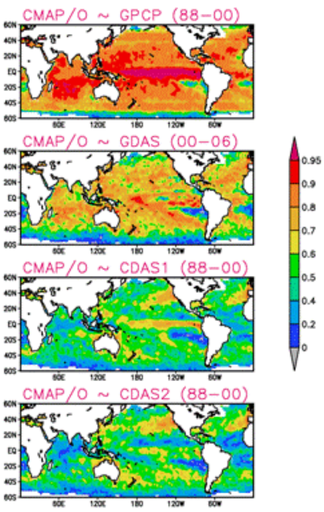

Fig. 8 Anomaly correlation between the monthly precipitation derived from a) the CMAP and GPCP (top); b) CMAP and GDAS (2nd from top); c) CMAP and CDAS1 (3rd from top); and d) CMAP and CDAS2 (bottom).

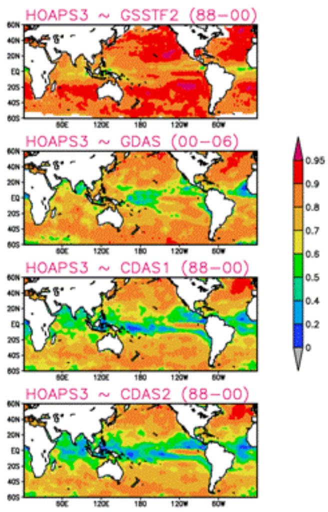

Fig.9 Anomaly correlation between monthly evaporation derived from a) the HOAPS3 and GSSTF2 (top); b) HOAPS3 and GDAS (2nd from top); c) HOAPS3 and CDAS1 (3rd from top); and d) HOAPS3 and CDAS2 (bottom).

In general, correlation between the observed data sets is very high (>0.8) over most of the global oceanic areas (top panels in fig.8-9), suggesting that individual observation-based data sets are capable of assessing the interannual variability of precipitation and evaporation of the NCEP model-based products with reliable accuracy. Anomaly correlation for CDAS1 and CDAS2 precipitation (fig.8) is above 0.5 over most of the global oceans and reaches 0.7 and higher over the areas covered by heavy precipitation (e.g. ITCZ and NW Pacific). Interannual variations of evaporation in the NCEP global products present good agreements with those of observations over most of the extra-tropical oceanic areas (fig.9). The NCEP operational GDAS generates precipitation and evaporation fields with better agreements with the observations than the CDAS1 and CDAS2, indicating potential of further improvements upon the current generation reanalyses through refined models and enhanced input observations. Substantial differences in the evaporation over the tropical oceans are attributable to multiple factors including differences in the state variables (surface wind, air temperature and humidity) and the bulk algorithms used to compute the evaporation in both the models and the observation-based data sets.

5. SUMMARY

1) Seasonal variations and interannual variability of oceanic precipitation and evaporation in NCEP CDAS1, CDAS2, GDAS, GFS and CFS are broadly consistent with observations;
2) GDAS presents the best performance among the five NCEP global products examined in this study;
3) However, consistent errors are observed in the fresh water flux fields generated by the NCEP rreanalyses and global models. In particular, the ITCZ is too weak in the CDAS1 and too strong in the GFS and GDAS, while evaporation in the CDAS2, GDAS, GFS and CFS is too large compared to the observations.

REFERENCES

Adler, R.F., and co-authors, 2003: The Version 2 Global Precipitation Climatology Project (GPCP) monthly precipitation analysis (1979 – present). J. Hydrometeor., **4**, 1147 – 1167.

Kalnay, E., and co-authros, 1996: The NCEP/NCAR 40-year Reanalysis Project. Bull. Amer. Meteor. Soc., 77, 437 – 472.

Chou, S.-H., E. Nelkin, J. Ardizzone, R. Atlas, and C.-L. Shie, 2003: Surface turbulent heat and momentum fluxes over global oceans based on the Goddard satellite retrievals, version 2 (GSSTF2). J. Climate, **16**, 3,256-3,273.

Grassl, H., V. Jost, J. Schulz, M.R. Ramesh Kumar, P. bauer, and P. Schluessel, 2000: The Hamburg Ocean-Atmosphere Parameter and Fluxes from Satellite Data (HOAPS): A climatological Atlas of satellite-derived air-sea interaction parameters over the World Oceans. Report No. 312, ISSN 0937-1060, Max Planck Institute for meteorology, Hamburg, pp.130 + figures.

Josey, S.A., E.C. Kent, and P.K. Taylor, 1998: The Southampton Oceanography Centre (SOC) Ocean – Atmosphere Heat, Momentum and Freshwater Flux Atlas. Southampton Oceanography Centre Rep. 6, 30pp + figures.

Josey, S.A., E.C. Kent, and P.K. Taylor, 1999: New insights into the ocean heat budget closure problem from analysis of the SOC air-sea flux climatology. J. Climate, **12**, 2850 – 2880.

Kanamitsu, M., W. Ebisuzaki, J. Woollen, S.-K. Yang, J.J. Hnilo, M. Fiorino, and G.L. Potter, 2002: NCEP-DOE AMIP-II Reanalysis (R-2). Bull. Amer. Meteor. Soc., **83**, 1631-1643.

Saha, S., S. Nadiga, C. Thiaw, J. Wang, W. Wang, Q. Zhang, H. M. van den Dool, H.-L. Pan, S. Moorthi, D. Behringer, D. Stokes, M. Pena, S. Lord, G. White, W. Ebisuzaki, P. Peng, P. Xie, 2006 : The NCEP Climate Forecast System. J. Climate, **19**, 3483-3517.

Tomita, H., M. Kubota, S. Iwasaki, T., Hihara, and A. Kawatsura, 2007: Introduction of J-OFURO version 2 surface heat flux data set and its analysis over the North Pacific. AGU 2007 Joint Assembly, Acapula, Mexico, May 22-25, 2007.

Xie, P., and P.A. Arkin, 1997: Global precipitation: A 17-year monthly analysis based on gauge observations, satellite estimates, and numerical model outputs. Bull. Amer. Meteor. Soc., **78**, 2539 – 2558.